HYBRID CONTROLLER FOR GUST LOAD ALLEVIATION AND RIDE COMFORT IMPROVEMENT USING DIRECT LIFT CONTROL FLAPS

Andreas Wildschek, Rudolf Maier*, Martin Hromcik**, Tomas Hanis**, Alexander Schirrer***, Martin Kozek***, Christian Westermayer***, and Mark Hemedi****

**EADS Innovation Works, Munich, 81663, Germany*

***Czech Technical University, Prague, 16627, Czech Republic*

****Vienna University of Technology, Vienna, 1040, Austria*

ABSTRACT

In this paper two robust H_∞ feedback control laws are designed, one for active wing bending damping, and one for active damping of the wing and hull bending modes. For the latter, not only symmetrically commanded ailerons are used, but also the elevator and direct lift control (DLC) flaps. The control objective of these feedback laws is the reduction of fatigue of the wing roots, as well as the improvement of ride comfort. Two different H_∞ control design methods, DK iteration and HIFOO, are applied and compared. For the additional compensation of turbulence excited peak loads, the active wing bending damper is augmented by an adaptive feed-forward controller which uses the modified output of an alpha probe mounted at the front fuselage as reference signal. Numeric simulations with a state-space model of the symmetric dynamics of a large airliner are performed for validation of the controllers' performances.

1. INTRODUCTION

Turbulent atmosphere, gusts, and manoeuvres significantly excite aircraft rigid body motions and, especially on large airliners, also structural vibrations, which leads to increased structural loads and reduced ride comfort. Today, large transport aircraft are commonly equipped with gust load alleviation systems. The objective of these control systems is the reduction of atmospheric turbulence excited dynamic loads, as well as an increase of passenger comfort and handling qualities. Robust feedback of structural accelerations to aerodynamic control surfaces has been proposed for active vibration damping in the past [1], [2].

A significant technological step forward is the work of HAHN & KOENIG [3] who successfully reduced turbulence excited vertical accelerations on the DLR Advanced Technologies Testing Aircraft (ATTAS) by using a feed-forward controller and direct lift control (DLC) flaps. Thereby, the aim was an improvement of passenger comfort. A modified alpha probe signal provided the reference for vertical turbulence. HECKER & HAHN [4] propose a similar feed-forward approach for gust load alleviation and ride comfort improvement on a large flexible airliner.

In WILDSCHEK [5] an adaptation algorithm is proposed for the feed-forward compensation of wing bending vibrations in order to make the control performance robust against plant uncertainties. Continuatively, a hybrid controller, i.e. the augmentation of active wing bending damping by feed-forward control is suggested for maximum alleviation of dynamic wing loads. Recently, said approach has been extended to the additional alleviation of turbulence excited pitch oscillations by using the elevators as actuators [6]. It is concluded, however, that the availability of additional DLC flaps would enable the simultaneous reduction of wing loads and improvement of ride comfort. In this paper a hybrid controller is designed for gust load alleviation and improvement of ride comfort on a large airliner using such DLC flaps in addition to the primary control surfaces such as elevators and ailerons.

2. AIRLINER MODEL WITH DIRECT LIFT CONTROL FLAPS

State-space models of symmetric dynamics of a large airliner for 4 different mass configurations and two different centre of gravity (CG) positions are used in this paper for the design of a hybrid controller for gust load alleviation and comfort improvement. Said models are in principle similar to the ones used in JEANNEAU ET AL. [2] and in WILDSCHEK [5], [6]. However, in addition to symmetrically commanded inner ailerons and the elevator, 3 pairs of direct lift control (DLC) flaps are modelled using the Doublet Lattice Method, compare Figure 1. For the following investigation the Mach number and altitude are considered to be available as gain scheduling parameters. Thus, the hybrid controller is only designed for the cruise Mach number and altitude.

All actuator dynamics are modelled by 2nd order low pass filters. Sensor delays and analogue filters are also considered. Moreover, a pitch damper consisting of a wash-out filter and a low pass filter is applied to the airliner model before design of the hybrid controller. The outputs of the models comprise CG pitch rate q_{CG}, vertical wing root bending moment Mx_{WR}, vertical root bending moment of the horizontal tail plane Mx_{HTP}, as well as vertical accelerations at several positions.

The control objective of the robust inner feedback control loop (which will be used for the hybrid controller) is the minimisation of the H∞ norm of a modal wing bending acceleration signal Nz_{law} as also proposed in JEANNEAU ET AL. [2] in order to reduce wing root fatigue loads. Said signal Nz_{law} is defined to be half of the sum of the vertical accelerations of the two wings Nz_{LW}, Nz_{RW} minus the vertical acceleration of the centre of gravity Nz_{CG}, see eq. (1) and Figure 1. This approach allows the separation of the vertical wing bending from the rigid body motion in the measurement.

$$Nz_{law} = \left[\frac{(Nz_{LW} + Nz_{RW})}{2} - Nz_{CG} \right] \tag{1}$$

For a second robust H∞ feedback controller design that seeks also active damping of the hull bending mode (which was found to be the critical for ride comfort), vertical accelerations at the pilot station Nz_{front}, at the CG, and at the rear fuselage Nz_{rear} are used to define a modal hull bending acceleration signal Nz_{hull}:

$$Nz_{hull} = \left[\frac{(Nz_{front} + Nz_{rear})}{2} - Nz_{CG} \right] \tag{2}$$

For control law design and evaluation in regards to ride comfort a comfort filter is applied to vertical fuselage accelerations as proposed in ISO2631, compare Figure 2 for a bode magnitude plot of this filter.

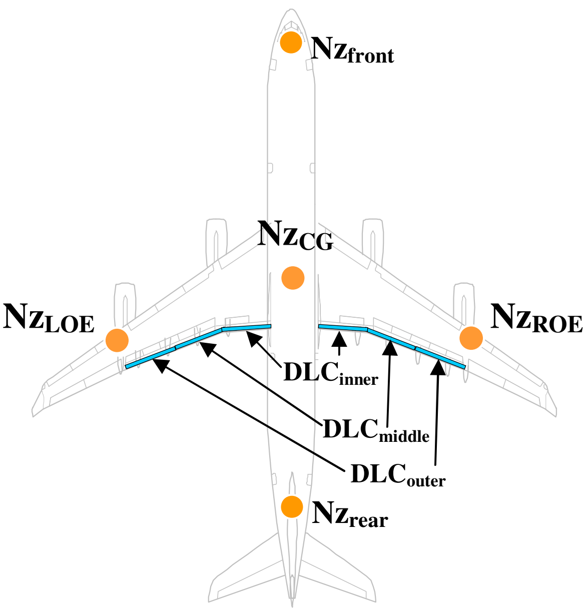

Figure 1: *Nz* acceleration sensors, DLC flap pairs.

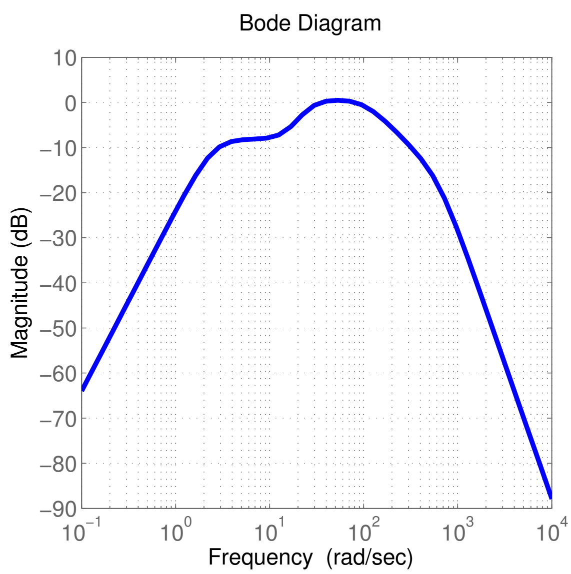

Figure 2: ISO2631 comfort filter for *Nz*.

3. DESIGN OF THE INNER FEEDBACK LOOP

Two modern approaches were considered for the design of the robust inner feedback loop, namely the DK iteration and a fixed-order H_∞ optimal control design using the HIFOO (H_∞ Fixed-Order Optimization) toolbox (see GUMUSSOY ET AL. [8]).

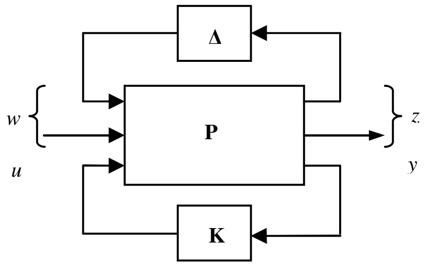

Figure 3: Generalized plant representation

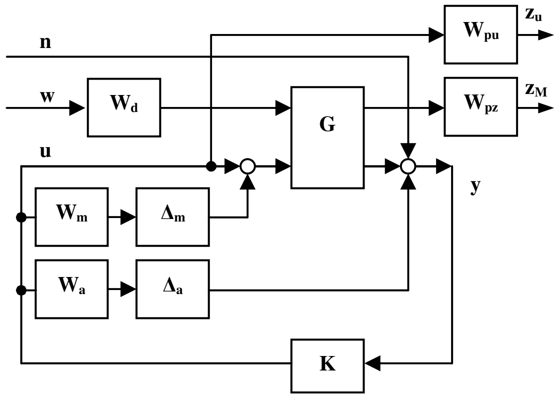

Figure 4: Design system for DK iteration

3.1. DK iteration

The DK iteration procedure is applied to obtain robust control laws that guarantee both robust stability and robust performance for an explicitly modelled set of uncertainties. The set of uncertain plants is formulated via the generalized $\mathbf{P}$-$\mathbf{\Delta}$ interconnection structure common in robust control design (see Figure 3). The derivation of the method is outlined in detail in SKOGESTAD AND POSTLETHWAITE [9] and utilizes the notion of the structured singular value μ in terms of the μ-analysis of robust stability / performance. The robust controller design algorithm alternately computes the H_∞-optimal controller design problem ($\mathbf{K}$-step) and the optimization for applied scaling matrices $\mathbf{D}$ to adapt for the considered and critical uncertainties. The algorithm seeks to minimize (bounds for) μ using the objective function

$$\min_{\mathbf{K}}\left(\inf_{\mathbf{D}\in\mathcal{D}}\left\|\mathbf{D}\mathbf{M}\mathbf{D}^{-1}\right\|_{\infty}\right), \qquad (3)$$

where $\mathbf{M}$ is the nominal closed loop with controller $\mathbf{K}$ and $\mathcal{D}$ is the set of all matrices $\mathbf{D}$ fulfilling $\mathbf{D}\mathbf{\Delta}\mathbf{D}^{-1}=\mathbf{\Delta}$).

Results were obtained for the aircraft model with the following control goals and choice of inputs and outputs:

- The chosen design task was active vibration damping of the aircraft subject to excitation by gust and turbulence. The primary goal was the damping of the first wing bending mode at a frequency of about 9 rad/s (1.4 Hz).
- The exogenous vertical wind input *w* is modelled as a white-noise signal filtered by a one-dimensional von Kármán turbulence spectrum.
- To obtain robustness with respect to measurement noise, an additional noise input *n* is modelled.
- The exogenous (performance) output z_M is the wing root bending moment. The first wing bending mode is also strongly distinct in the transfer function from the wind input to the wing bending acceleration signal Nz_{law}, and is therefore also a possible performance output. However, if manoeuvre load control is a further design goal, a load performance output is advantageous to the modal sensor.
- The measurement output (controller input) *y* is the wing bending acceleration signal Nz_{law}.
- As control input *u* the symmetrically commanded inner ailerons are used, showing the strongest effect of all available control surfaces on the wing bending mode.

- The plant model is furthermore extended by uncertainties for actuator deviation (multiplicative input uncertainty), neglected dynamics between validation and design models (additive uncertainty), as well as performance design weights. The resulting design system is depicted in Figure 4.

3.1.1. Choosing design weights and tuning performance

The chosen weights are combinations of band-pass and notch-filters around the wing bending frequencies. In order to design a controller to attenuate the first wing bending mode, the performance weight is high at that frequency, while the additive uncertainty weight is reduced there using a notch filter. The second wing bending mode lies in some mass cases very close to the hull bending mode (at around 17 rad/s or 2.7 Hz), which requires a weight parameter search to optimize for both robustness and performance for all validation mass/CG cases. It was found that an uncertainty peak at 16.7rad/s successfully yields a controller which is robust and performs well in all validation cases. Moreover, actuator uncertainties were modelled as multiplicative input uncertainty with constant magnitude of W_m=0.05, and actuator magnitude limitation was obtained by control input performance weights (unity for W_{pu} for control input magnitude limitation and a tuned design weight W_{pz}). Measurement noise is modelled by white noise *n*, and the turbulence excitation is implemented using white noise *w* and the turbulence spectrum shaping in W_d.

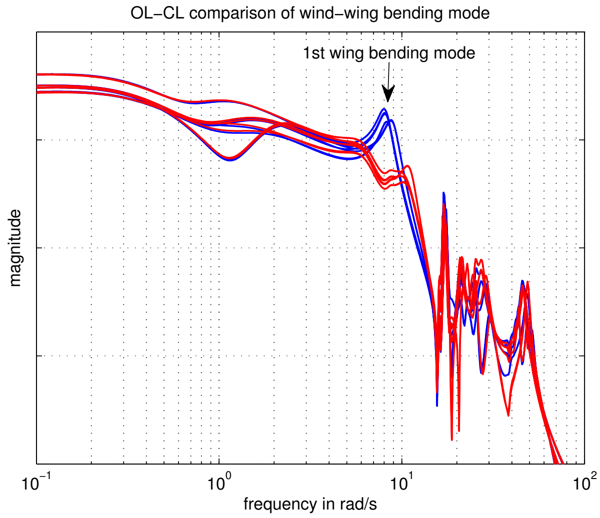

Figure 5: Comparison of the wind – wing root bending moment transfer functions for all validation plants, open loop (blue lines) and closed loop (red lines) using the robust DK iteration controller

The resulting SISO controller is robust for all mass/CG cases and successfully attenuates the wing bending mode and, to a small extent, the second wing bending mode (at around 17 rad/s or 2.7 Hz), while having little or no influence at other frequencies. Due to the resulting high controller order, subsequent controller order reduction is required before implementation. It also became evident that the inner ailerons suffer large phase uncertainty with respect to mass/CG variations in the frequency range of the second wing bending and hull bending mode (17 .. 20 rad/s or 2.7 .. 3 Hz), so a MIMO approach was also taken in the following.

3.2. Fixed-order H∞ optimal control design using HIFOO (H∞ Fixed-Order Optimization)

In order to directly obtain a robust feedback controller of pre-specified order, the H∞ Fixed-Order Optimization (HIFOO) toolbox is used, outlined in detail in GUMUSSOY ET AL. [8]. The HIFOO control design method searches for locally optimal solutions of a non-smooth optimization problem that is built to incorporate minimization objectives and constraints for multiple plants. First, the controller order is fixed at the outset, allowing for low-order controller design. Second, no Lyapunov or lifting variables are introduced to deal with the conflicting specifications. The resulting optimization problem is formulated on the controller coefficients only, resulting in a typically small-dimensional non-smooth non-convex optimization problem that does not require the solution of large convex sub-problems, relieving the computational burden typical for Lyapunov LMI techniques. Because finding the global minimum of this optimization problem may be hard, an algorithm that searches only for local minima is used. While no guarantee can be given on the result quality of this algorithm, in practice it is often possible to determine a satisfying controller efficiently.

A MIMO low-order H∞-optimal controller was computed aiming at the following goals and requirements:

- Robust damping of the wing bending mode (WBM) and hull bending mode (HBM) for reduction of fatigue loads and for comfort improvement
- Low-order controller, robust with respect to the entire set of validation plants

The control architecture is chosen as MIMO feedback control with 2 performance outputs (wing root bending moment Mx_{WR}, horizontal tail plane bending moment Mx_{HTP}), 2 measurement outputs (i.e., controller inputs – the modal wing bending sensor Nz_{law} and the modal hull bending sensor Nz_{hull}) and all actuators being commanded by the controller.

3.2.1 Performance criteria definition

The weighting filters used to represent performance criteria are defined according to the requirements and constrains for the control law as listed above. The selected filters are mostly combinations of band-pass and notch-filters to ensure WBM and HBM suppression. The shape of the performance criteria can by slightly modified for a particular plant (according to natural frequency shift and changes in mode damping) in order to exactly fulfil the performance for all mass/CG cases. The resulting controller achieves considerable reductions of the first WBM and the HBM at very low controller order. However, this MIMO concept requires further careful fine-tuning in order to reduce spill-over into other modes.

Design Method →	DK iteration	Fixed-order HIFOO design
Robustness	explicit uncertainty model (robustness for the defined uncertain plant set)	vertex robustness (robustness for a number of design plants)
Computational effort	computationally fast (consecutive convex computations)	computationally fast (for local optimization) / high (for more relevant results)
Controller design	high control order (plant order + 2 x **D** scales order)	arbitrarily low controller order

Table 1: Properties of the applied robust control design methods

4. DESIGN OF THE ADAPTIVE FEED-FORWARD AUGMENTATION

The feed-forward controller uses the elevator, the symmetrically commanded ailerons, and the symmetrically commanded DLC flaps as actuators. The control objective of the feed-forward augmentation is the minimisation of a quadratic cost function *J*, defined as:

$$J = \left\langle {Nz_{law}}^2 + {Nz_{hull}}^2 + \left(ISO \cdot \Delta Nz_{CG}\right)^2 \right\rangle \tag{4}$$

The transfer function of the comfort filter denoted *ISO* is used to weigh the vertical CG acceleration Nz_{CG} according to relevancy for comfort. This has the additional advantage that the low frequency range where the transfer path from DLC flaps to Nz_{CG} is completely uncertain is cut off. In order to avoid an adaptation towards unwanted compensation of pilot inputs, vertical CG accelerations are minimized in terms of *deviations* from pilot commands $Nz_{CG_{pilot}}$:

$$\Delta Nz_{CG} = Nz_{CG} - Nz_{CG_{pilot}} \tag{5}$$

The feed-forward controller is adapted online in order to improve its performance robustness against plant uncertainties, as described in WILDSCHEK & MAIER [6]. Using only one reference sensor (i.e. the alpha probe), the discrete-time feed-forward control law for the *m*th actuator u_m at time step *n* is:

$$u_m(n) = \vec{h}_m(n)^T \cdot \vec{\alpha}(n) = \vec{\alpha}^T(n) \cdot \vec{h}_m(n) \qquad m = 1,2,3 \tag{6}$$

with *m*th FIR (Finite Impulse Response) control filter:

$$\vec{h}_m(n) = \left[h_{0_m}(n), h_{1_m}(n), \ldots, h_{N-1_m}(n)\right]^T \quad m = 1,2,3 \tag{7}$$

Thereby, $h_{0_m}(n), h_{1_m}(n), ..., h_{N-1_m}(n)$ are the coefficients of the m^{th} FIR control filter, and *N* denotes the control filter length, which is assumed to be equal for all three controllers for the sake of straightforwardness of notation. $\vec{\alpha}(n)$ is the vector of the sampled reference signal at time step *n*:

$$\vec{\alpha}(n) = [\alpha(n), \alpha(n-1), ..., \alpha(n-N+1)]^T \tag{8}$$

The frequency domain steepest descent update law for the m^{th} FIR control filter is:

$$\vec{h}_m(n) = \vec{h}_m(n-1) - c \cdot IDFT \left\{ \sum_{l=1}^{L} \left[\hat{R}_{lm}^*(n, f_k) E_l(n, f_k) \right] \right\}_+ \tag{9}$$

Thereby, $IDFT\{...\}_+$ denotes the causal share of the Inverse Discrete Fourier Transform of the quantity inside {..} with f_k denoting the discrete frequency. The superscript * denotes complex conjugation and *c* is the convergence coefficient. Contrary to [6], but as illustrated in ELLIOT [7], only one common convergence coefficient is chosen in order to avoid distortion of the gradient of the cost function *J*. Then $\hat{R}_{lm}(n, f_k)$ is the Discrete Fourier Transform (DFT) of the latest 2*N*-point segment of the sampled *estimated* filtered reference signal $\hat{r}_{lm}$, which is the sampled reference signal $\vec{\alpha}$ filtered by the transfer path $\hat{G}_{lm}$. Thereby, $\hat{G}_{lm}$ is an estimate of the plant's transfer path from the m^{th} control command u_m to the l^{th} error signal e_l, which is denoted G_{lm}. Furthermore, $E_l(n, f_k)$ is the 2*N*-point DFT of the latest *N* point segment of e_l padded with *N* zeros. Finally, only the causal share of the quantity inside the brackets {..} is used. This approach is called *overlap-save method* and prevents circular correlation.

5. SIMULATION RESULTS

Numeric simulations were performed with state space models of the symmetric dynamics of a large airliner. An alpha probe modelled at the aircraft's front fuselage was used as a reference sensor for feed-forward control. For the simulations, the reference signal, i.e. the modified alpha probe signal, is denoted α_{sim}.

$$\alpha_{sim}(t) = \alpha_{wind}(t) + \alpha_{ground}(t) = \alpha_{air}(t) - \alpha_0(t) \tag{10}$$

It is composed of two parts, namely α_{wind} which is generated by von-Kármán-filtered white noise and represents atmospheric turbulence, and α_{ground} which is the output of the state space model representing the movement of the alpha probe's mounting node in the air stream due to aircraft rigid body motions and structural vibrations. The required reference signal is α_{wind}. Therefore, any significant α_{ground} has to be compensated in the alpha probe output, such as proposed in [3] and [4]. The main share of α_{ground} stems from the aircraft rigid body motion which are mainly excited by pilot inputs. Since in the numeric simulations no pilot inputs were considered, α_{ground} was so small that it can be neglected in the derivation of the adaptation algorithm. The unfiltered alpha probe measurement is denoted α_{air}. It is assumed that the mean value α_0 is removed, e.g. by a high pass filter. The turbulence excitation of the aircraft was modelled as span-wise constant angle of attack variation α_w.

$$\alpha_w = \alpha_{wind} + \alpha_v \tag{11}$$

Thereby an angle of attack α_v is added to the observable share of the turbulence excitation α_{wind} in order to represent the coherence degradation between reference measurement and turbulence exciting the wing. For small angles $\alpha_{wind} = v_z / V_{TAS}$ (in radians) holds. Thereby, the vertical flow velocity v_z shall represent the one-dimensional von Kármán turbulence spectrum. For the time-domain simulations the von Kármán turbulence spectrum is approximated by filtering a white noise signal by a 3rd order filter with the integral scale length chosen as 762 meter. In order to achieve 75% coherence between reference measurement α_{sim} and the aircraft excitation (which is an appropriate estimate for the excitation of the first symmetric vertical wing bending on a large airliner as explained in [5]), α_v is von-Kármán-filtered white noise which is uncorrelated to α_{wind} (different initial seeds in the simulation) with a magnitude ratio of $|\alpha_v| / |\alpha_{wind}| = \sqrt{1/3}$

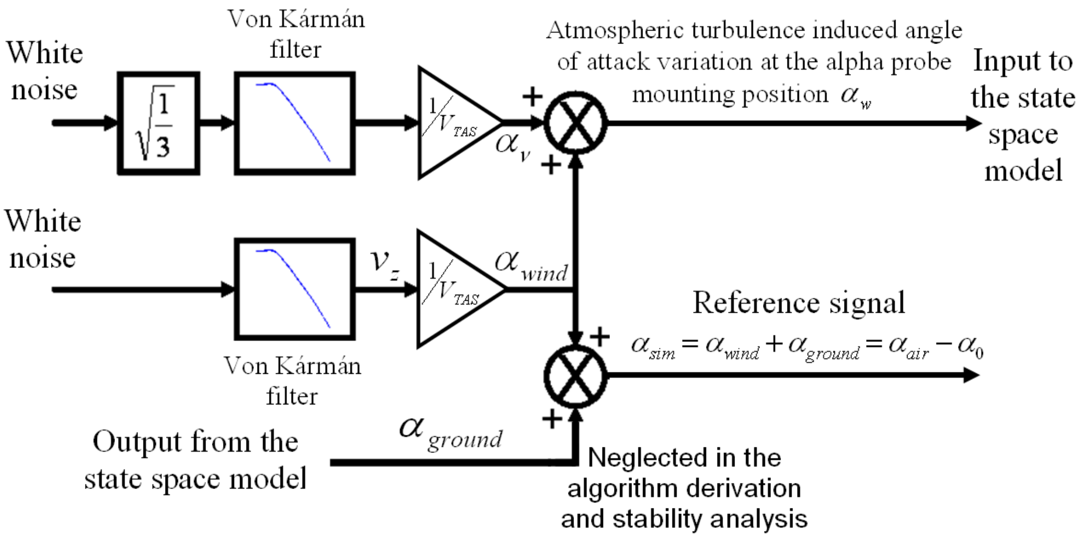

Figure 6: Modelling of turbulence excitation and turbulence measurement with 75% coherence between reference measurement and aircraft excitation [5].

In Figure 7 magnitudes of the outputs of the airliner model at the design mass case/CG position are illustrated with turned off controller (blue lines), with a HIFOO feedback controller aiming at active damping of the wing bending and hull bending mode (red lines), and with a hybrid controller, i.e. inner feedback controller from Nz_{law} to the inner ailerons designed by DK iteration, mainly for active wing bending damping, augmented by an adaptive feed-forward controller that commands the inner ailerons, the elevator and the DLC flaps (green lines).

All controllers achieve a reduction of Nz_{law} at the first symmetric vertical wing bending frequency (i.e. between 1 and 1.5 Hz), and thus also reduce the wing root bending moment Mx_{WR} in this frequency range. However, this does not necessarily imply that peak loads are reduced. The pitch rate q_{CG} and the tail plane bending moment Mx_{HTP} remain largely untouched. The HIFOO feedback controller also attenuates the hull bending mode significantly (top right plot), thus reducing Nz_{CG}, as well as the vertical accelerations in the front and the back of the fuselage weighted by the ISO2631 comfort filter (denoted $ISO \cdot Nz_{front}$ and $ISO \cdot Nz_{rear}$) especially in the frequency range of the first vertical hull bending mode, i.e. between 3 Hz and 4 Hz. This leads to a significant improvement of ride comfort. Active damping of the hull bending mode seems to be the most promising approach for ride comfort improvement in this frequency range. Here the main challenges are the uncertainty of the plant dynamics of these frequencies and the high computational burden for real-time control.

The hybrid controller (green lines) shows only little improvement of ride comfort in the frequency range between 3 Hz and 4 Hz. Additional damping of the hull bending mode most probably will improve this situation. The main advantage of the additional feed-forward path used in the hybrid control concept however is the reduction of peak loads in the wing roots, see Figure 8, which, in theory, allows for a lighter design of the wing structure. Note that in this case the feed-forward controller becomes safety critical. The time response to von Kármán turbulence excitation shows that the peak loads of the wing root bending moment Mx_{WR} are reduced without increasing the peaks of the horizontal tail plane bending moment Mx_{HTP}. Additionally, the maxima of pitch rate q_{CG} and vertical accelerations in the fuselage are reduced by feed-forward control.

The main challenge with feed-forward control is to provide a reliable reference signal. On the large airliner investigated in this paper wing bending vibration acceleration magnitude can be reduced to 50% by pure feed-forward control when an alpha probe mounted at the front fuselage is used as a reference sensor (as also shown in [5]).

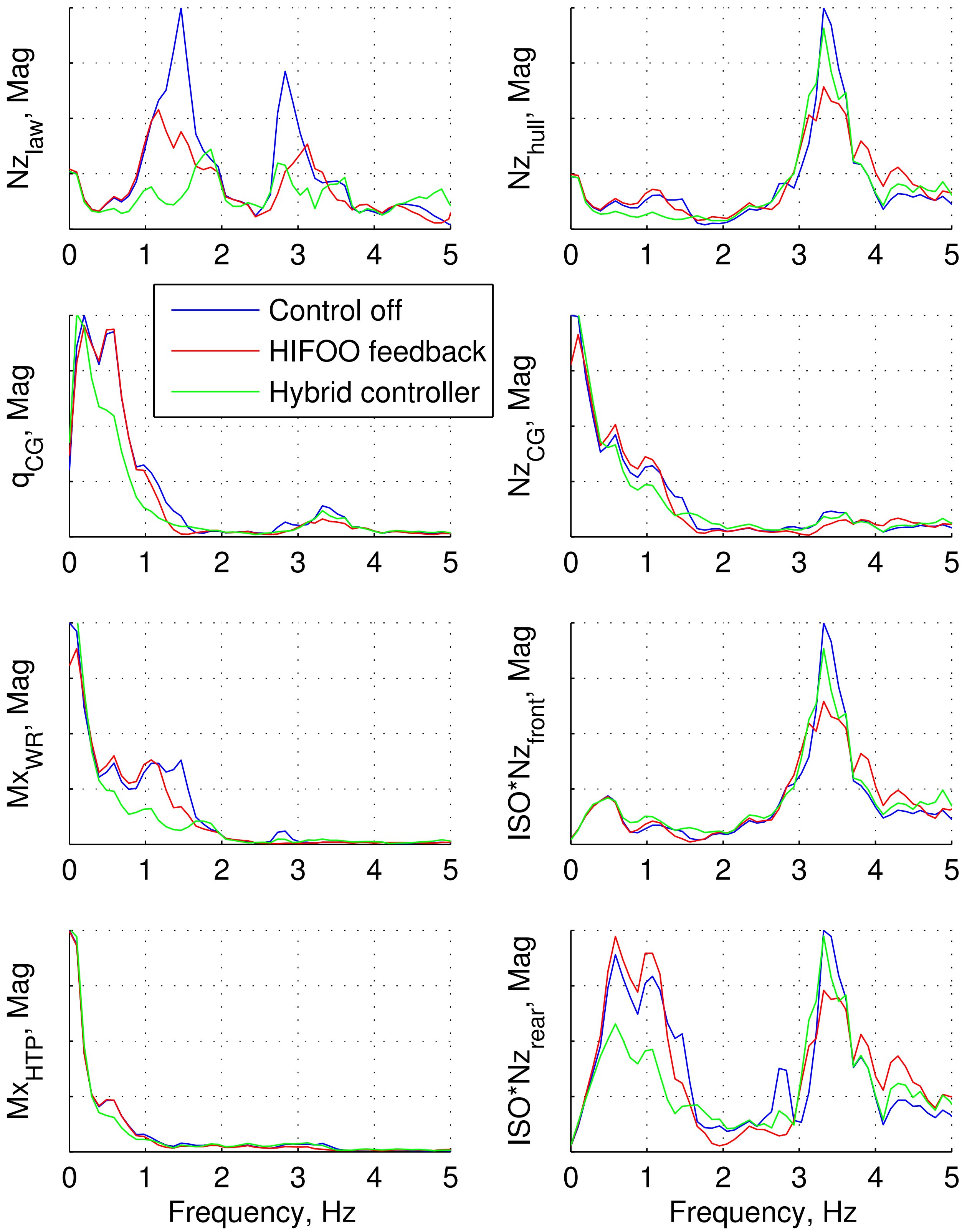

Figure 7: Magnitudes of aircraft model outputs with different controllers for one mass/CG case.

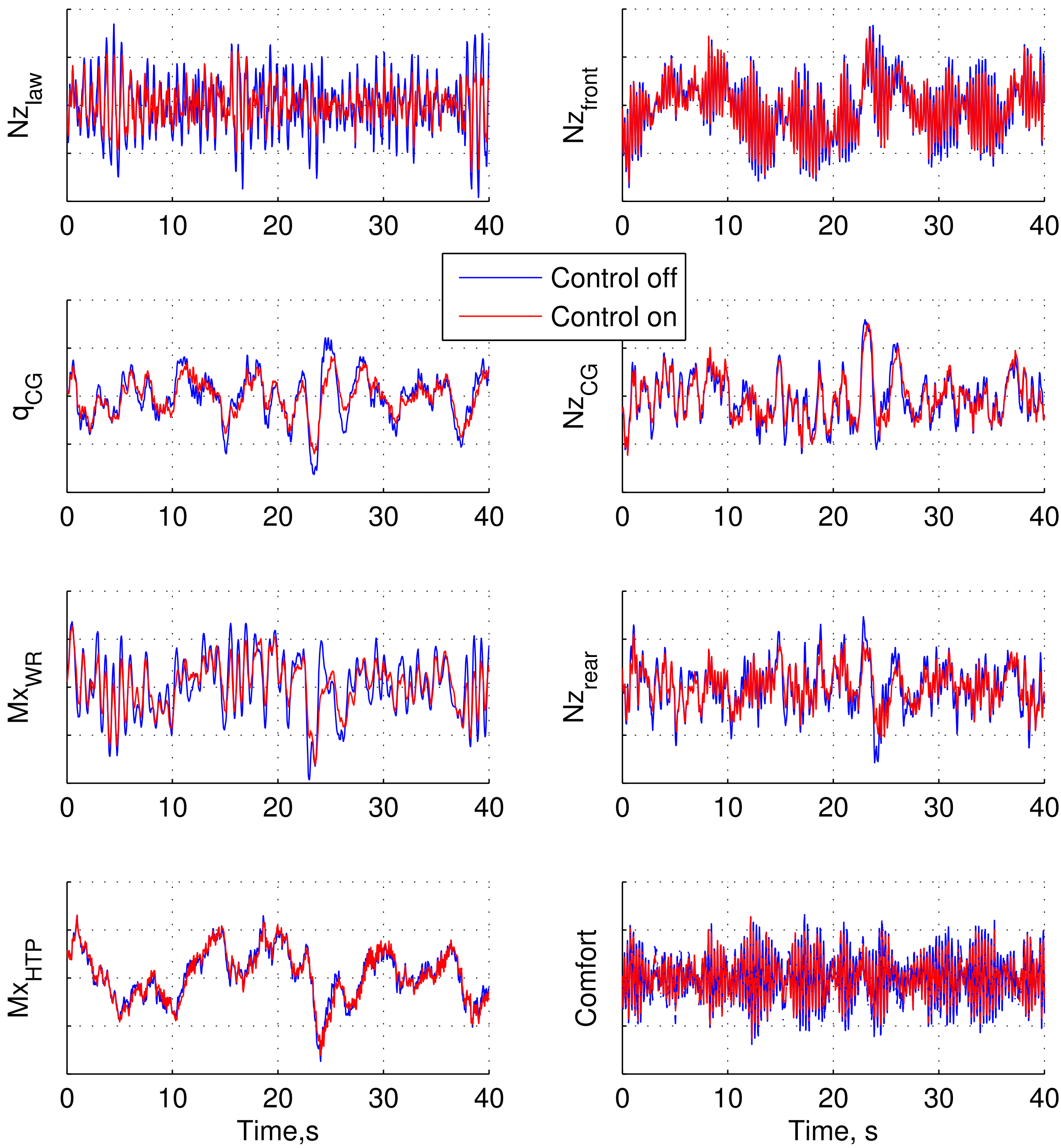

Figure 8: Reduction of peak loads with the converged adaptive feed-forward controller.

6. CONCLUSIONS

Hybrid control, that is, a combination of robust feedback wing bending damping and adaptive feed-forward compensation of turbulence excitation is proposed for gust load alleviation. The overall objective is the reduction of the dynamic wing root bending moment and fatigue loads, as well as an improvement of ride comfort, which is evaluated with an ISO2631 comfort filter. All available control surfaces (elevators, symmetrically commanded ailerons, and symmetrically commanded direct lift control (DLC) flaps) serve as actuators. The design of the inner feedback loop for active wing bending damping is performed by DK iteration. The proposed adaptive feed-forward concept is applied to the feedback-controlled closed loop system. The adaptation improves the performance robustness of the feed-forward path against plant uncertainties. Peak loads in the wing root are reduced by the feed-forward path, thus opening the possibility of a lighter design of the wing structure. Comfort improvement is very good in the frequency range of first vertical wing bending, but low in the frequency range of the hull bending mode. Note also that the resulting high order of the robust H_∞ feedback controller still needs to be reduced before implementation.

In order to improve comfort also in the frequency range of the hull bending mode an alternative robust MIMO feedback controller for active damping of the wing and hull bending mode using all control surfaces is designed. This time also a low controller order is sought which can be achieved by using the H_∞ fixed order optimization (HIFOO) toolbox. It can be shown that active damping of the hull bending mode indeed is the most efficient means for ride comfort improvement.

These two approaches are validated in numeric simulations with state space models of the longitudinal dynamics of a large airliner. The excitation is modelled as one-dimensional von Kármán turbulence.

A next step would be to tune the HIFOO feedback controller to reduce spill-over and to augment it with the adaptive feed-forward concept for additional reduction of wing root peak loads.
Manoeuvre load alleviation is currently under investigation. In a given pitch-up manoeuvre, for example, the inner DLC flap pair is deflected downwards, so that less (upward) deflection of the elevator is required in order to perform said manoeuvre. This procedure is assumed to dramatically decrease the manoeuvre wing root bending moment. Control laws for manoeuvre load alleviation are in the design phase. However, no results are yet available.

REFERENCES

[1] JOHNSTON, J. F., ET AL., Accelerated Development and Flight Evaluation of Active Controls Concepts for Subsonic Transport Aircraft Volume 1 – Load Alleviation/Extended Span Development and Flight Test. NASA CR-159097, pages 2-11, 1979.

[2] JEANNEAU, M., AVERSA, N., DELANNOY, S., HOCKENHULL, M., Awiator's study of a Wing Load Control: Design and Flight-test Results. *16th IFAC Symposium on Automatic Control in Aerospace*, St. Petersburg (RUSSIA), 14-18 June 2004.

[3] HAHN, K.-U. KOENIG, R., ATTAS flight test and simulation results of the advanced gust management system LARS. In *AIAA Atmospheric Flight Mechanics Conference*, Hilton Head Island, SC, Aug 10-12, 1992.

[4] HECKER, S., HAHN, K.-U., Advanced Gust Load Alleviation System for Large Flexible Aircraft, 1st CEAS European Air & Space Conference, Berlin, Germany, 10.-13. September, 2007.

[5] WILDSCHEK, A., An Adaptive Feed-Forward Controller for Active Wing Bending Vibration Alleviation on Large Transport Aircraft, Dissertation, Technische Universität München, 2009.

[6] WILDSCHEK, A., MAIER, R., Integrated Adaptive Feed-forward Control of Atmospheric Turbulence excited Rigid Body Motions and Structural Vibrations on a Large Transport Aircraft. In *American Control Conference 2008*, Seattle, Washington, June 11-13, 2008.

[7] ELLIOTT, S. J., Signal Processing for Active Control, Academic Press, London, 2001, page 247 ff.

[8] GUMUSSOY, S., HENRION, D., MILLSTONE, M., OVERTON, M., Multiobjective Robust Control with HIFOO 2.0, to be registered as a LAAS-CNRS Research Report, January 2009. IFAC Symposium on Robust Control Design, Haifa, Israel, June 16-18, 2009.

[9] SKOGESTAD, S., POSTLETHWAITE, I., Multivariable Feedback Control Analysis and Design, John Wiley & Sons Ltd, 1996.